LASER INTERFEROMETER GRAVITATIONAL WAVE OBSERVATORY

LIGO Laboratory / LIGO Scientific Collaboration

LIGO- T050204-00 ADVANCED LIGO OCTOBER 9, 2005

Wireless optical controls of Ligo static suspensions actuators

Maria Paola Clarizia *, Riccardo Desalvo, Calum I. Torrie

Distribution of this document:
LIGO Science Collaboration

This is an internal working note
of the LIGO Project.

California Institute of Technology

LIGO Project – MS 18-34
1200 E. California Blvd.
Pasadena, CA 91125
Phone (626) 395-2129
Fax (626) 304-9 834
E-mail: info@ligo.caltech.edu

Massachusetts Institute of Technology

LIGO Project – NW17-161
175 Albany St
Cambridge, MA 02139
Phone (617) 253-4824
Fax (617) 253-7014
E-mail: info@ligo.mit.edu

LIGO Hanford Observatory

P.O. Box 1970
Mail Stop S9-02
Richland WA 99352
Phone 509-372-8106
Fax 509-372-8137

LIGO Livingston Observatory

P.O. Box 940
Livingston, LA 70754
Phone 225-686-3100
Fax 225-686-7189

http://www.ligo.caltech.edu/

* University of Sannio, Palazzo Bosco Lucarelli, corso Garibaldi 107, 82100 Benevento Italy .

Maria Paola Clarizia
maripa83@yahoo.it

FINAL REPORT 09-23-2005

Wireless optical controls of Ligo static suspensions actuators [1]

1.1 THE SUSPENSION SYSTEM OF ADVANCED LIGO AND THE AIM OF THIS PROJECT

Seismic noise is one of the main problems to face when dealing with interferometric detectors. At very low frequencies, seismic motions dominate the detectors' noise, degrading their sensitivity, and negatively affecting the detection. One of the main goals of Advanced Ligo is to improve the efficiency of the suspension attitude control system, which determines the isolation of the mirrors used in the interferometric detectors from the noise platform. The suspension system of Advanced Ligo consists of sophisticated multi-stage multi-pendulum attenuators that isolate the test masses from local ground motions: the one used for Advanced Ligo has an improved efficiency since a single pendulum has been replaced by a quadruple pendulum. The figure below shows a schematic diagram and a picture of the suspension system.

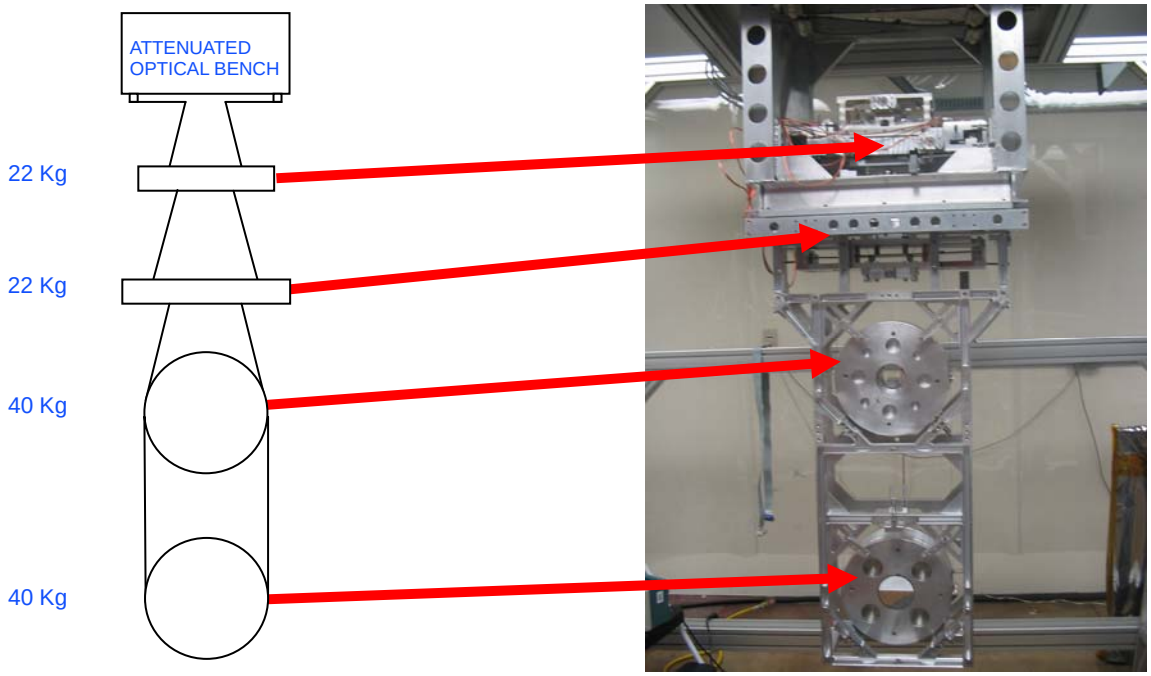

Figure 1.1.1: schematic diagram and picture of a prototype suspension system like the one that will be used for Advanced LIGO

The suspension system includes a tuning mass, shown in the following pictures, which is placed on the top of the four masses of the quadruple pendulum: this mass plays a very important role since moving it forward and backward allows us to control the pitch of the masses and so of the mirror itself, and this means that one can control and adjust the static displacement of the laser beam simply rotating the tuning mass.

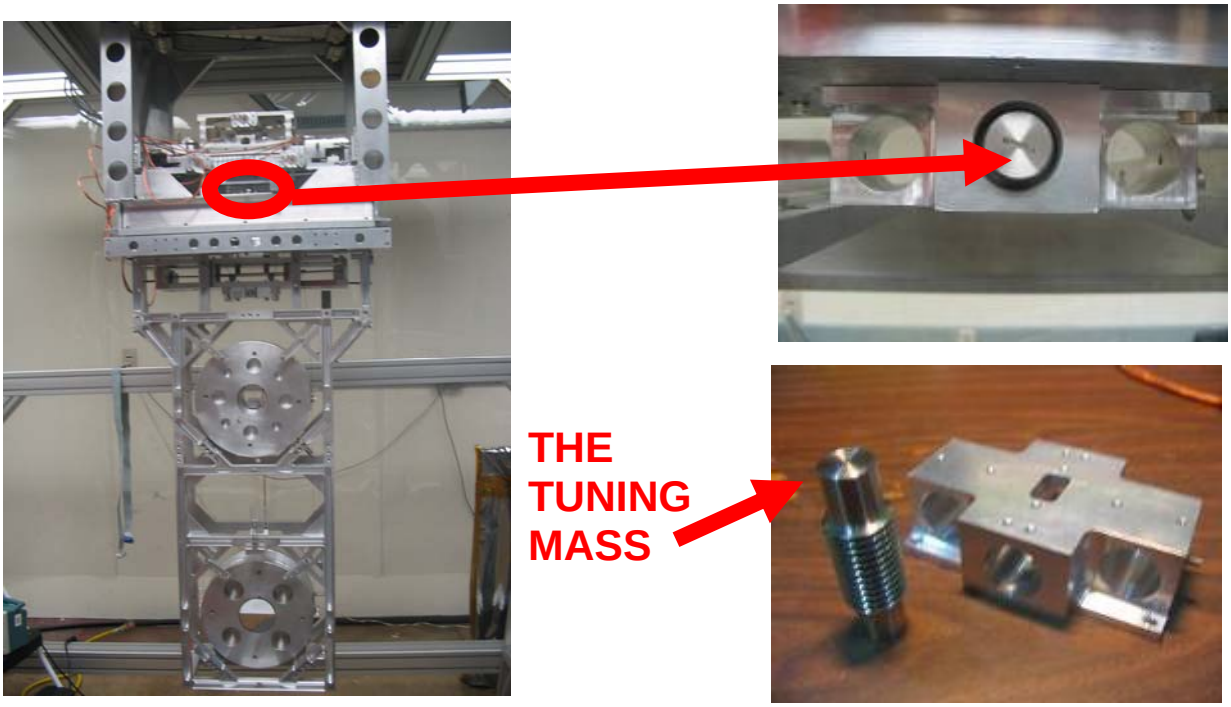

Figure 1.1.2: some photographs of the tuning mass used to tilt the mirror

At present, the tuning mass is moved manually, but a problem arises when the tank is closed, since there will be no access in it and a manual tuning will not be possible. The solution to this problem is to make a remote control of the pitch of the mirror, and this can be done replacing the tuning mass with a stepper motor, and controlling it remotely from outside. The stepping motor would move its own mass my means of a threaded shaft, offering a mechanized way of adjusting the mirror when the access to the vacuum chamber is not possible.
The aim of this work is then to improve the efficiency of the adjusting operations mentioned before by using a stepping motor. The stepping motor will be fed and controlled by a wireless circuit, so as to eliminate mechanical and electrical perturbations on the suspended masses, which would derive from the use of a wired link, as well as an excessive load of outgas on vacuum: in this way, optimization of such operations is achieved without introducing further noises. Figure 1.1.3 shows some sketches of the actual system, with the present tuning mass, and the proposed one, where the mass will be replaced by a stepping motor.

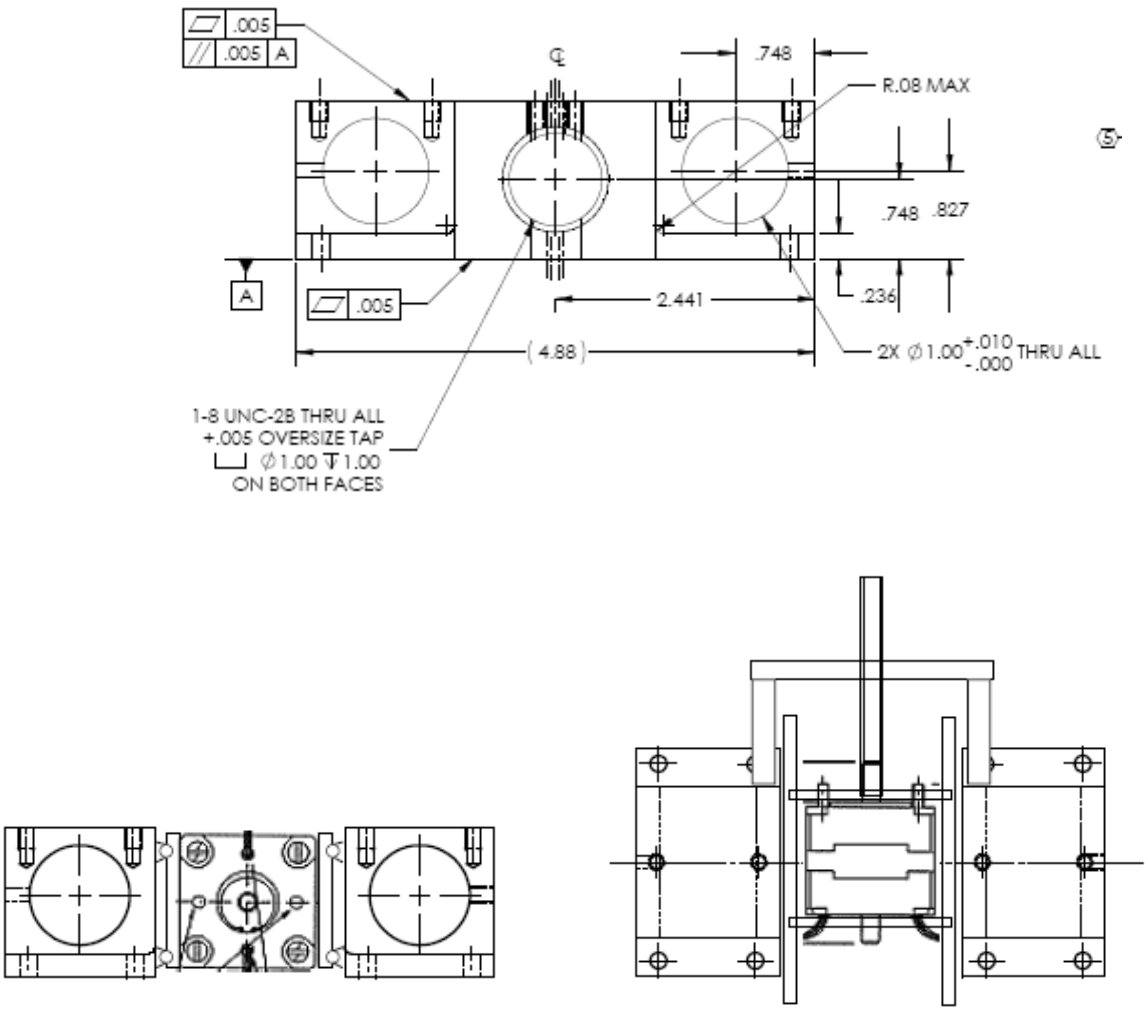

Figure 1.1.3: sketches of the present system, where a tuning mass is used to tilt the mirror, and the proposed one, where a stepping motor will replace the tuning mass

1.2 THE STEPPING MOTORS AND ITS CHARACTERISTICS

A stepping motor, whose picture is shown below, is an electric motor that rotates in small discrete steps (tipically 1.6°), and it's used when something has to be positioned very precisely or rotated by an exact angle [1].

Figure 1.2.1: a photograph of examples of stepping motors

In a stepper motor, a moving part, the internal rotor, containing permanent magnets is controlled by a static part, the stator, which consists of a set of stationary electromagnets that are switched electronically and a suitably shaped magnetic flux return geometry that presents 200 stable positions equally spaced over the 360^{o} of the stator rotation, corresponding to the steps. Hence, it is a cross between a DC electric motor and a solenoid. The structure of a stepping motor is shown in figure 1.2.2.

Figure 1.2.2: an example of stator and rotor of a stepping motor

When one of the electromagnets is charged, the nearest teeth are attracted by the magnetic field, pulling the rotor to a given direction and making a step. The procedure is then repeated, as shown in figure 1.2.3. Of course no step happens if the magnetic “gear” is already lined with the electromagnet which is being activated. The desired motion is obtained by exciting the four coils of the motor in a suitable sequence.

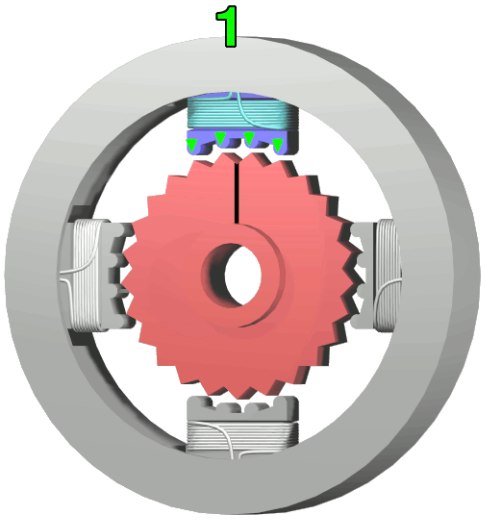

The top electromagnet (1) is charged, attracting the topmost four teeth of a sprocket.

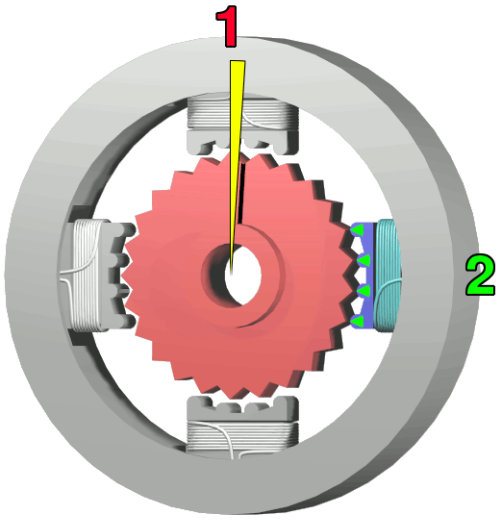

The top electromagnet (1) is turned off, and the right electromagnet (2) is charged, pulling the nearest four teeth to the right. This results in a rotation of 3.6°.

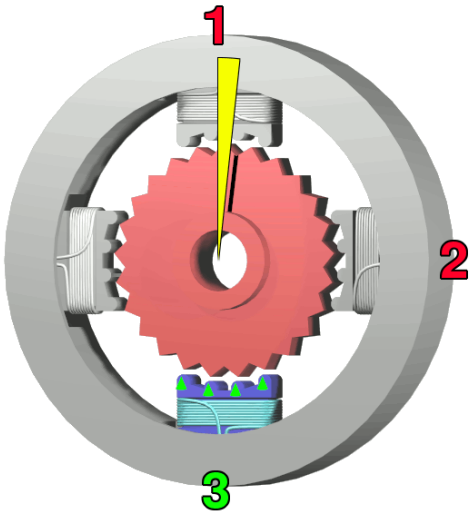

The bottom electromagnet (3) is charged; another 3.6° rotation occurs.

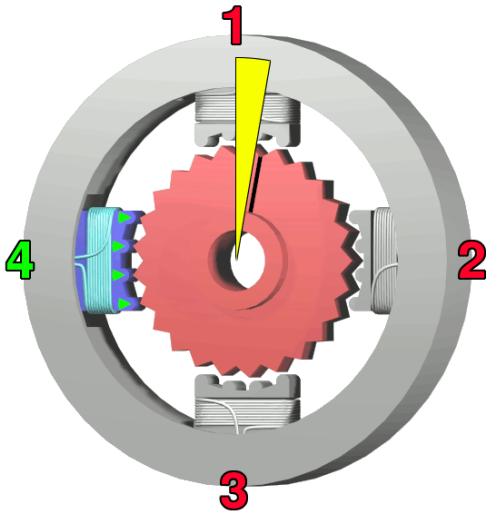

The left electromagnet (4) is enabled, rotating again by 3.6°. When the top electromagnet (1) is again charged, the teeth in the sprocket will have rotated by one tooth position; since there are 25 teeth, it will take 100 steps to make a full rotation.

Figure 1.2.3: a representation of how a motor works

Stepper motors have a fixed number of magnetic poles that determine the number of steps per

revolution. Most common stepper motors have 200 full steps/revolution, meaning it takes 200 full steps to turn one revolution. Advanced stepper motor controllers can utilize pulse-width modulation to perform microsteps, achieving higher position resolution and smoother operation. Some microstepping controllers can increase the step resolution from 200 steps/rev to 50,000 microsteps/rev.
Stepper motors are rated by the torque they produce. A unique feature of steppers is their ability to provide position holding torque while not in motion. Since their aim is to keep the rotor still, they make a step to reach a certain angular position when they are activated, and they maintain that position. To achieve full rated torque, the coils in a stepper motor must reach their full rated current during each step.
The motor can also make steps sending bursts of current into its coils, following a pre-determined sequence. The motor used for this project has four coils (eight wires), which have been two by two connected to get a two coil configuration (figure 1.2.4) and fed according to the sequence shown in the table 1: a burst of current is injected into the two coils to produce the first two steps, and then the same current with opposite sign, is used to make the last two steps.

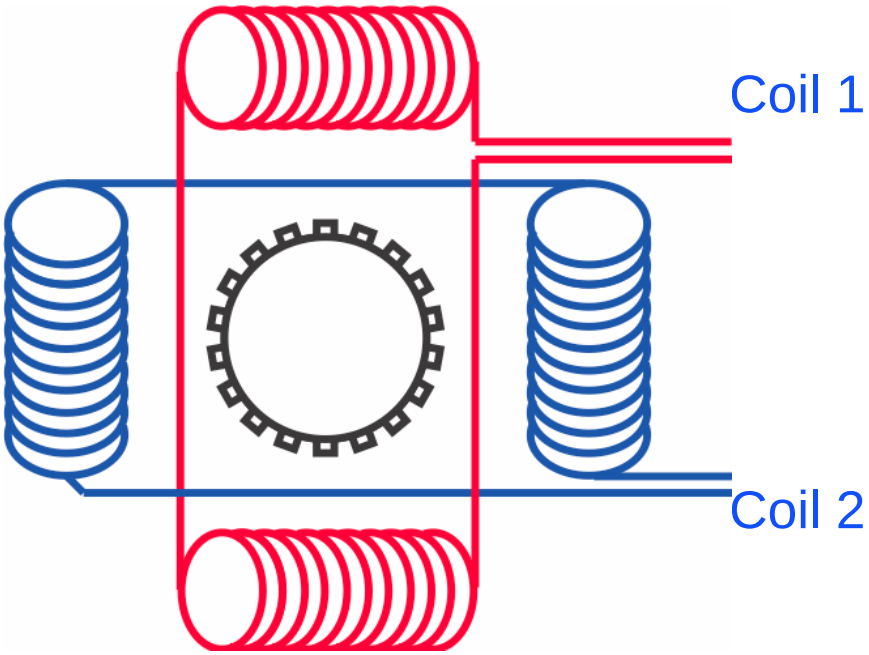

Figure 1.2.4: a representation of the coils of a motor

Steps	Coil 1	Coil 2
1	+ i	
2		+ i
3	- i	
4		- i

Table 1: the sequence used to make steps with a 2-coil motor

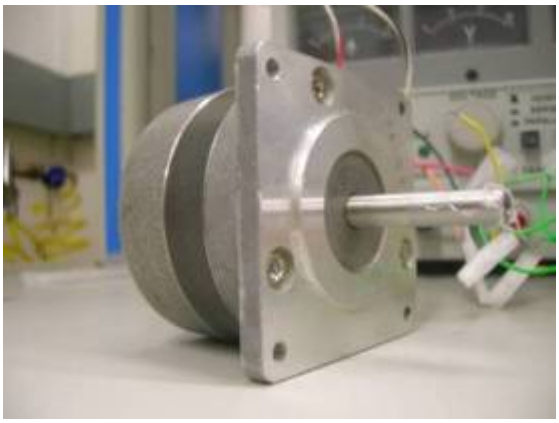

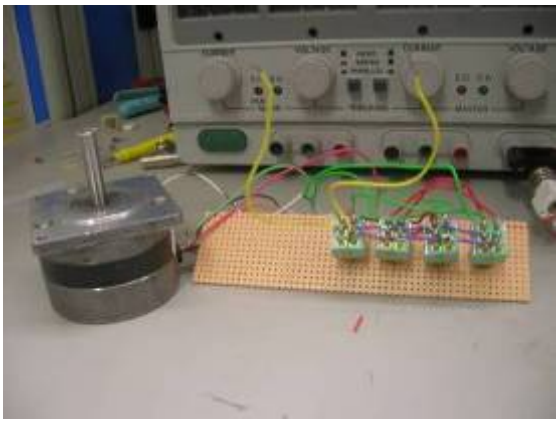

Figure 1.2.5: photographs of the motor used for this experiment

The pictures above show the motor used for this project. It nominally requires a voltage supply of 3.6 volts. The first step of the experiment is to test its operation using a capacitor and switches. The procedure to test it is the following: a charge is stored in the capacitor, and then a burst of current is injected in each of the coils of the motor, according to the sequence shown in the table above, by means of pushbutton switches.

The motor really used for the suspension system of Advanced Ligo, shown in figure 1.2.6, is an UHV (Ultra-High Vacuum) stepper motor, manufactured by AML motor, which is one of main manufacturer of vacuum-compatible stepper motors. Due to its good features and performance, this kind of motor has been proposed to replace the tuning mass in the suspension system: further specifications are available on the web [3].

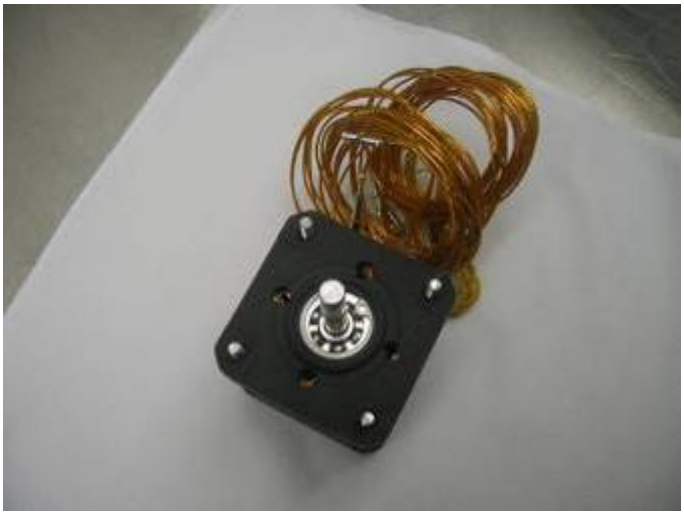

Figure 1.2.6: a photograph of the stepping motor which may replace the tuning mass of the suspension system for Advanced LIGO

1.3 THE FEEDING CIRCUIT

The wireless circuit used to control the motor consists of a chopped laser and a photodiode to generate an ac voltage that can be stepped up with a transformer, and then rectified. The resulting dc voltage charges up a capacitor, which is used to produce a current which is injected into the coils of the motor by means of switches. A schematic diagram of the circuit and a picture of the real one are shown below.

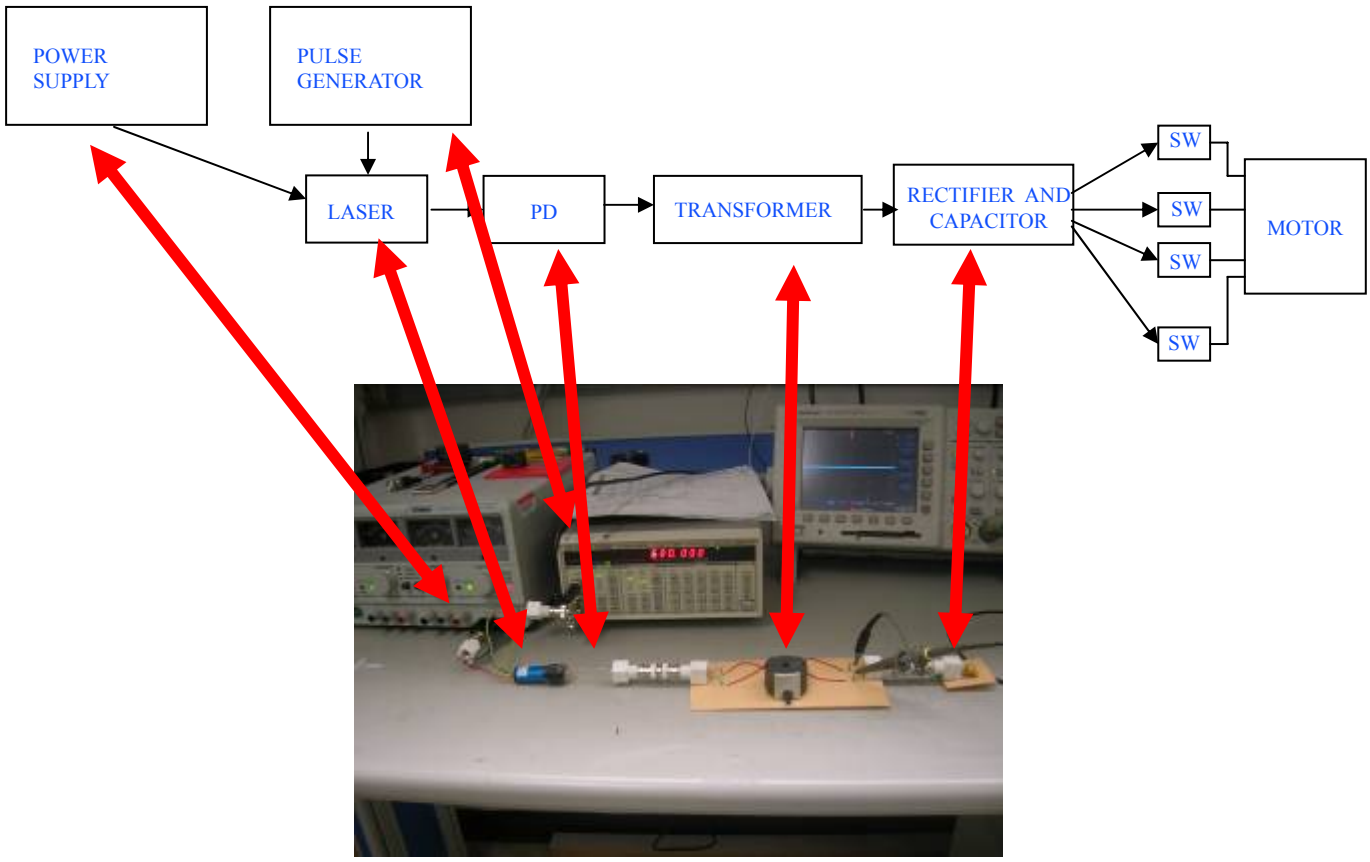

Figure 1.3.1: a schematic diagram and a picture of the wireless circuit used to feed the motor

1.3.1 The laser and the photodiode

The laser output signal can be modulated with any arbitrary waveform. The laser, shown in figure 1.3.1.1, has been connected to a power supply and a signal generator. The signal used is a square wave with amplitude 4 V and variable frequency. In real life the laser would be coupled to the diode via a telescope through vacuum view port. In this experiment the laser is coupled directly to the photodiode.
The laser used has a control frequency which goes from DC to 300 kHz, and an output power of 1 mW at a wavelength of 635 nm.
We chose a 1 mW laser for safety reasons (I was not qualified for high power lasers). In real life

a much more powerful laser would be used.

Figure 1.3.1.1: a picture of the laser connected to the photodiode

The silicon photodiode detector has a responsitivity of 0.42 A/W at a wavelength of 635 nm. The maximum output current of the detector is about 0.42 mA.

1.3.2 The transformer

the voltage obtained is still too low to feed a motor, a transformer is needed to step it up. A picture of a transformer (one of many) is shown in figure 1.3.2.1.

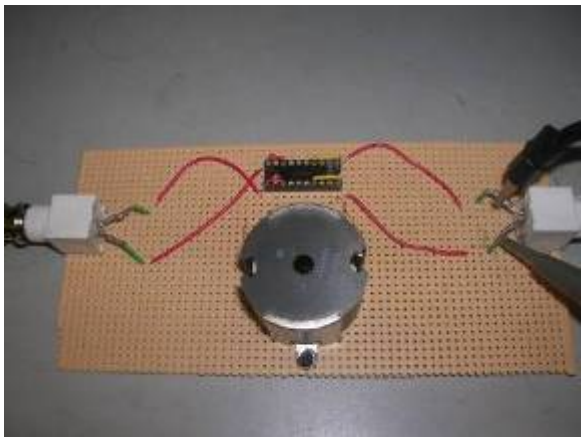

Figure 1.3.2.1: a picture of a transformer, whose primary and secondary are connected to two BNC connectors.

From theory we know that the ratio of the voltages on the primary and secondary is equal to the ratio of the number of the wires, and it is the inverse of the ratio of the current, but actually the search for the optimal transformer is not so simple and a lot of parameters play important roles.

$$\frac{V_1}{V_2} = \frac{N_1}{N_2} = \frac{I_2}{I_1}$$

One of the behaviors that has been empirically noted is that there are strong dependencies on the wire choice, the section of the core, and the excitation frequency. Particularly it has been verified that increasing the section of the core, the frequency corresponding to the maximum voltage decreases. This is probably due to the fact that the flux density of the produced magnetic field is proportional to the peak voltage developed across the winding and it is inversely proportional to the number of turns, to the frequency and to the cross-sectional area of the core [4]. For this reason, if the section of the core is increased, the frequency has to decrease to keep the flux density unchanged.
The search for a good transformer has been empirically accomplished, building a lot of transformers (as shown in figure 1.3.2.2) with different sections, turns on the primary and secondary and different turns ratios, and trying to obtain the highest voltage possible on the secondary winding.

Figure 1.3.2.2: a picture of me building transformer with the machine

The highest voltage resulted from a transformer with 200 coils on the primary and 1200 coils on the secondary. The wave obtained is represented in figure 1.3.2.3: it is almost totally positive, and the obtained peak to peak voltage is almost 20 V.

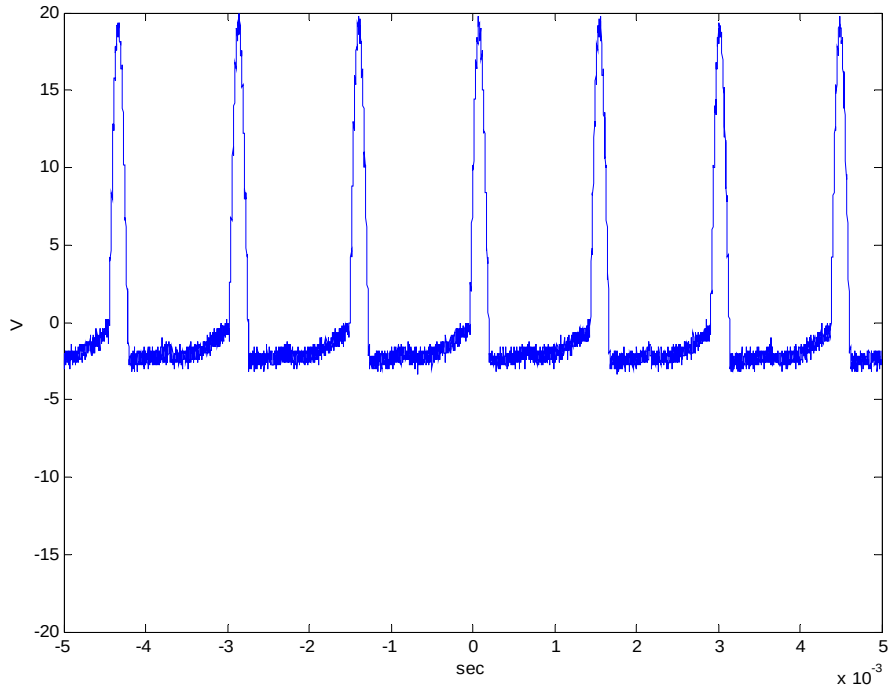

Figure 1.3.2.3: the signal coming from the secondary of the transformer used for the experiment

1.3.3 The rectifier

The rectifier used, whose schematic diagram is shown in figure 1.3.3.1, gives a DC voltage which is almost the peak to peak voltage of the wave coming from the transformer.

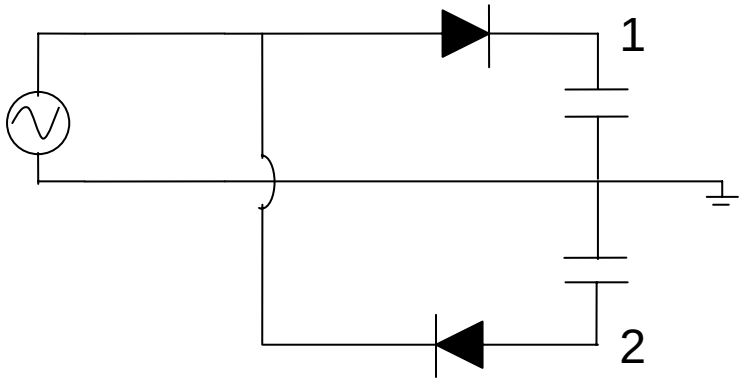

Figure 1.3.3.1: a schematic diagram of the rectifier used.

A little voltage drop is due to the diodes: the ones used are germanium diodes, which have a lower voltage drop in comparison to other kind of diodes. Moreover, since the waveform

obtained from the transformer is almost totally positive, the output voltage used for the motor has been taken between terminal 1 and the mass, instead of terminals 1 e 2, in order to use a smaller capacitor and then to have a smaller charge up time.

1.4 IMPEDANCE MATCHING

Problems of impedance matching were found because the rectifier impedance changes while the capacitor charges up. The figure 1.3.4.1 shows some representations of the voltage on the secondary of the transformer in different moments of the charging up of the capacitor. Voltage changes are clearly caused by impedance changes at the end of the circuit.

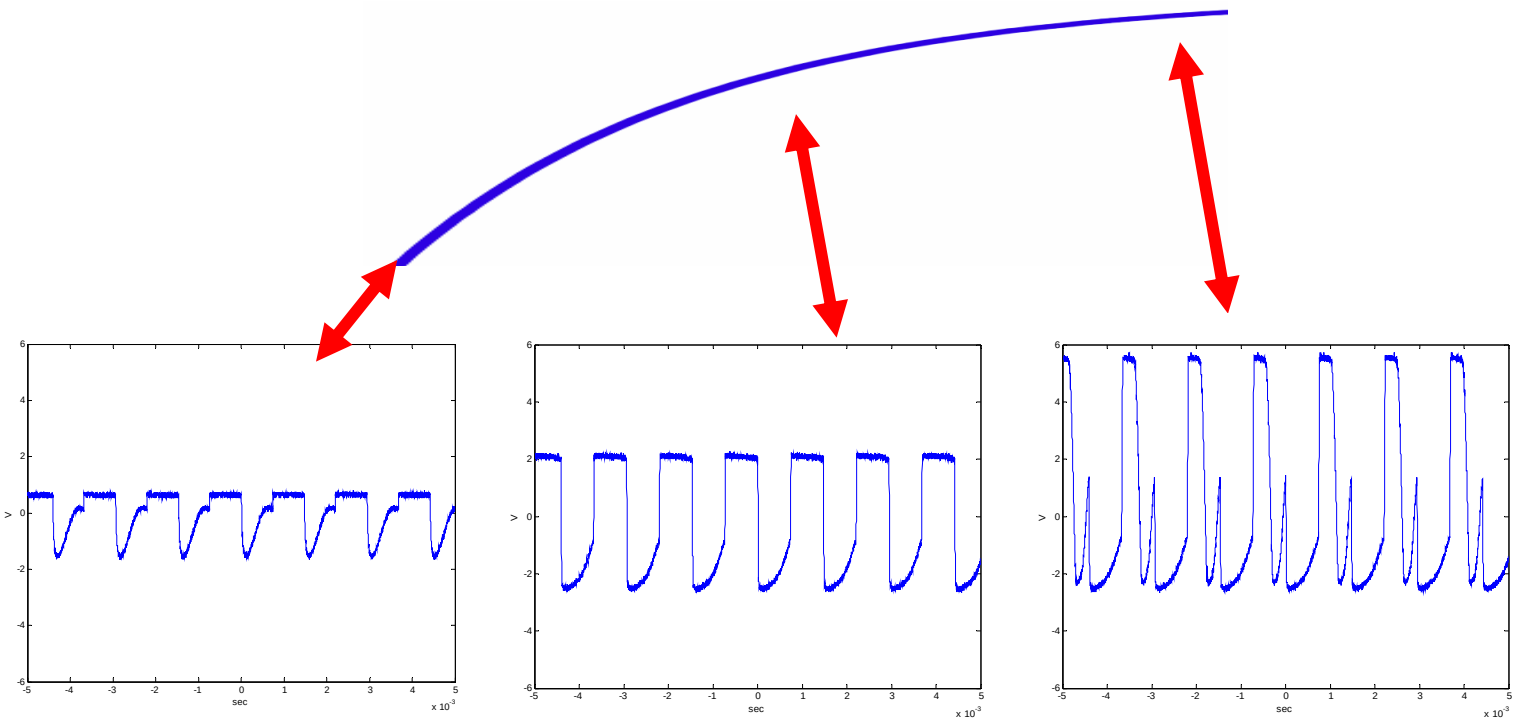

Figure 1.3.4.1: a representation of the changing voltage of the secondary during the charging up of the capacitor

1.5 THE CHOICE OF THE CAPACITOR

The generation of a motor step requires a certain amount of current, and then a certain amount of charge: the bigger the capacitance, the slower the charging up time, but the smaller the capacitance, the higher the voltage required for a motor step. Furthermore a capacitance larger

than the minimum necessary to generate a step would be preferable to defeat stictions. In normal operation a step would be commanded as soon as the capacitor has reached a sufficient voltage. In case of stiction (after long periods of inaction) a voltage higher than the one normally required is achieved by a longer charge up time to make the motor work again. Some measurements of different charge up times for different transformers and capacitances have been done to figure out which value of capacitance is the best one in terms of time and voltage. A capacitor of 100 microfarad turned out to be a good trade off: the voltage needed to move the motor is 5 volts and the time of wait for one step is about 1 minute (with our small laser). The figure 1.5.1 shows the behaviour of the capacitor chosen for the experiment.

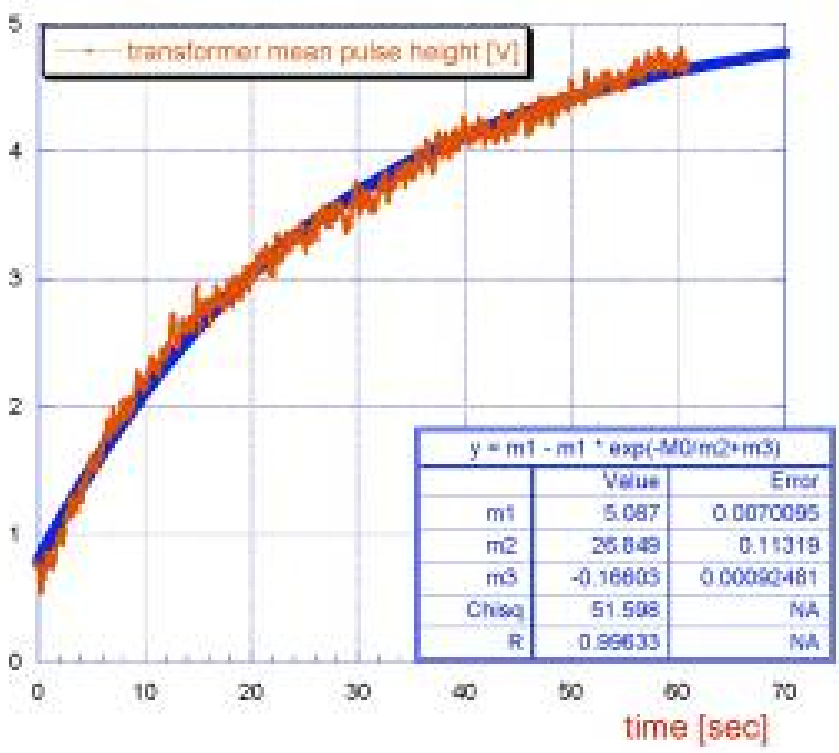

Figure 1.5.1: the charging curve of the capacitor chosen

1.6 IMPLEMENTATION IN A SUSPENSION SYSTEM

After having designed and tested the whole circuit, the next step would be to implement it in a suspension system.. The laser will be left outside the vacuum chamber and would be coupled to the diode via a telescope through a vacuum view port (figure 1.6.1).

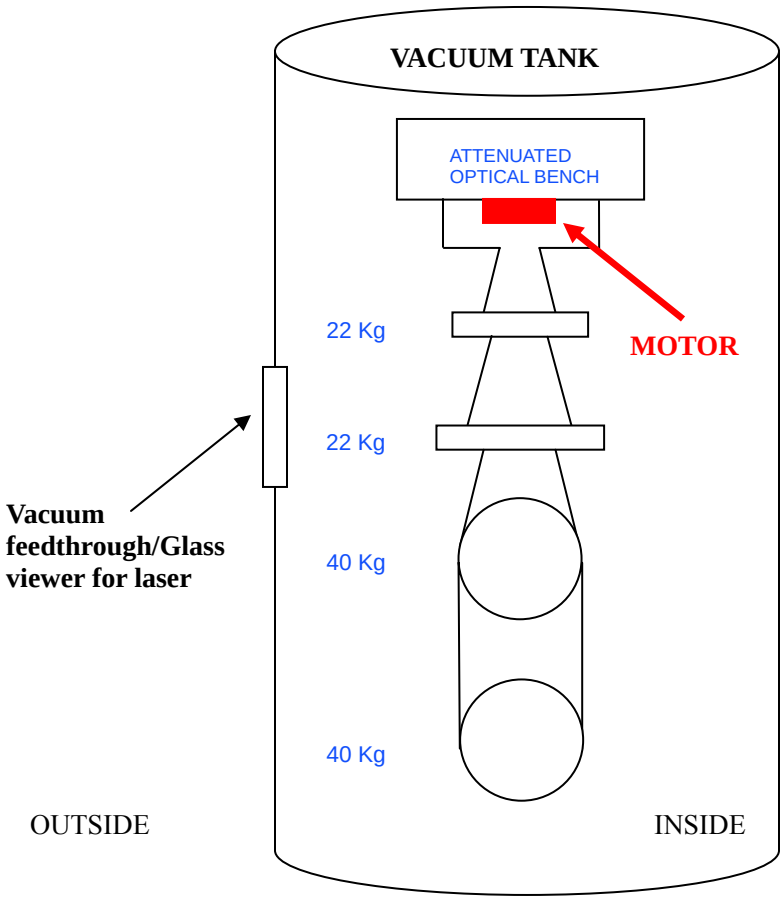

Figure 1.6.1: a sketch of the suspension system, with some elements placed inside and outside the vacuum tank

The laser will be aligned to the photodiode, placed inside the vacuum tank, together with the other components that form the feeding circuit (figure 1.6.2). Each single component has to be carefully chosen, so as to obtain a vacuum-compatible circuit: for instance, the capacitor cannot be electrolytic, since this kind of capacitors could cause outgassing phenomena; a ceramic capacitor is surely preferred in order to avoid this problem.

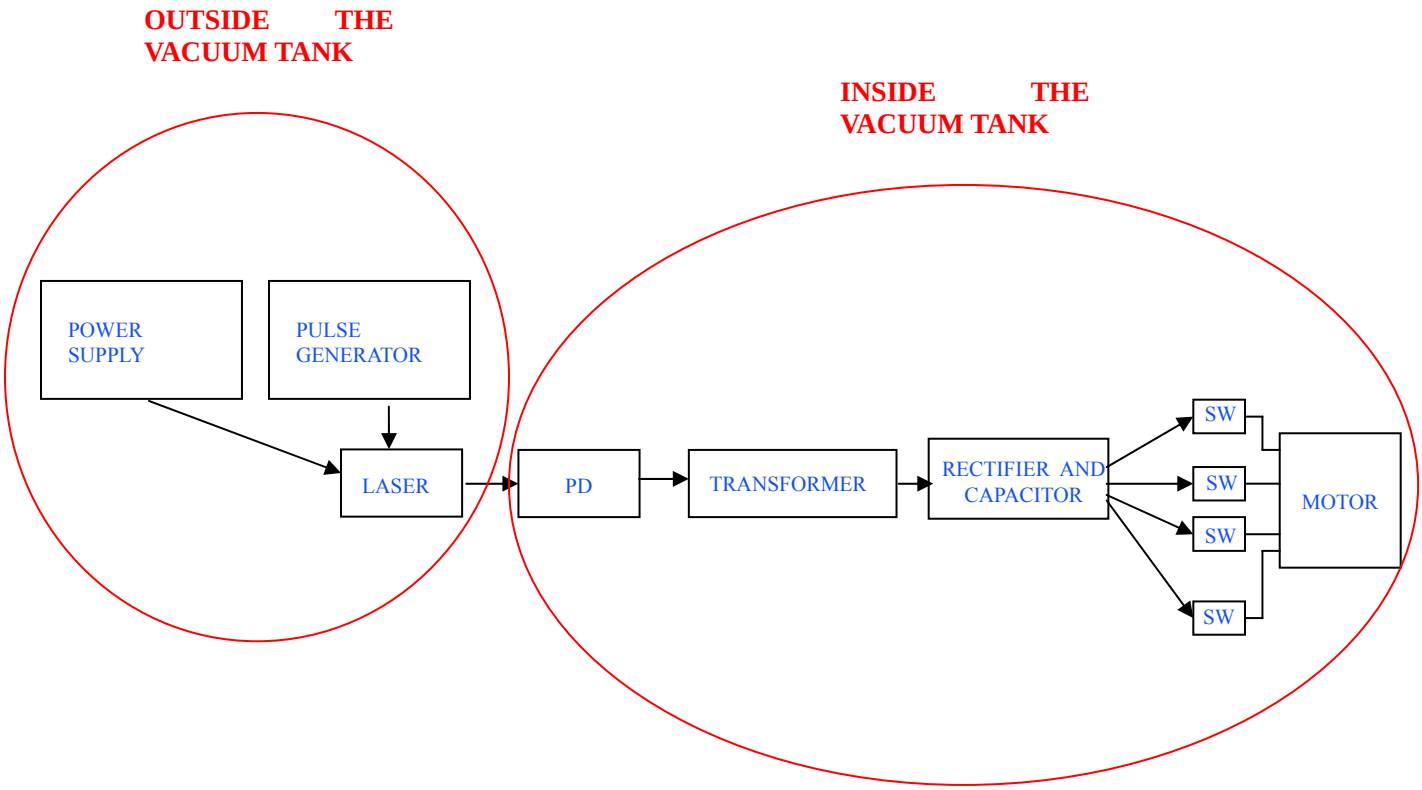

Figure 1.6.2: a sketch of the whole feeding circuit, where components placed outside the vacuum chamber are distinguished from the ones placed inside the vacuum chamber.

1.7 STARTING THE OPTICAL CONTROL OF THE MOTOR THROUGH THE USE OF FET SWITCHES

The next steps of the project will be the development of the FET switch control circuit of the motor: the principle is to use frequency jumps to control the gates of the FET switches and four bandpass filters to route the current pulses into the various coils of the motor, so as to control the number and the directions of the steps.
Some initial tests have been done to see how to implement the control circuit, using manual switches to control the FET gates.
Firstly, one of the motor coils has been connected to the drain of a FET switch, controlled by a 2.5 V voltage (chosen according to the FET specs) and a pushbutton switch. The voltage required to make a step has been provided to the coil through an RC circuit, and a large value resistance has been placed between the gate and the source (connected to the ground) of the FET switch, to shut down the FET when the switch is released, as shown in figure 1.7.1. When a voltage of 18 V is applied to the terminal A of the circuit, and a probe connected to an oscilloscope is placed onto the terminal B, we can see on the oscilloscope that the voltage goes down from about 18 V to almost 0 V when pushing the button, as expected, given the fact that the FET behaves like a short circuit and a current passes through the coil to cause a step.

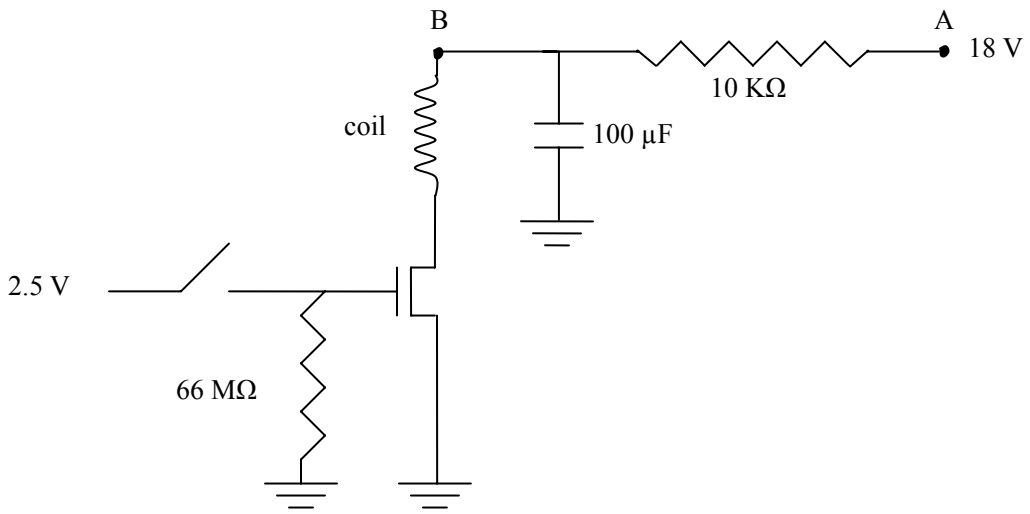

Figure 1.7.1: a sketch of how to use one FET to feed a coil of the motor

Current has to be injected into the coils in two directions to make steps clockwise and counterclockwise. A configuration using four FETs, has been designed to do that . It could be implemented to ensure the proper working of the motor. A simple test was performed with the same circuit as before, but using two FETs, to figure out which voltage is needed to feed the motor when using more than one FET. A sketch of this first configuration is shown in figure 1.7.2.

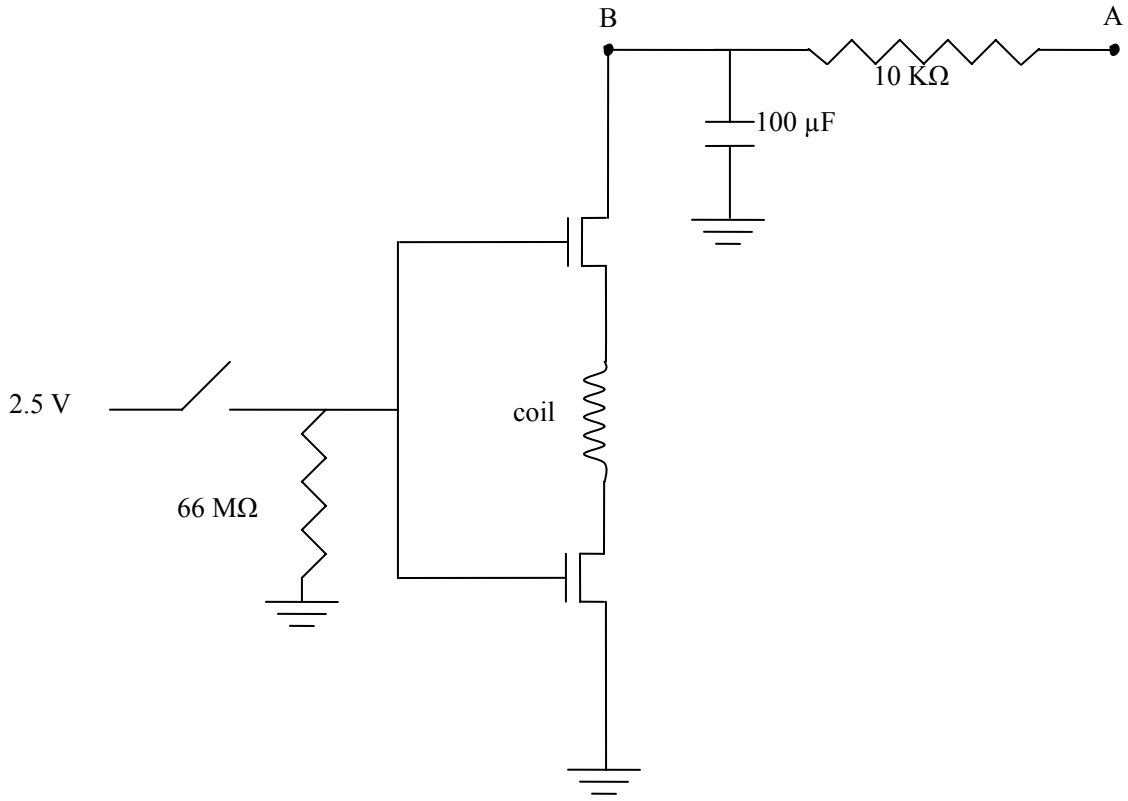

Figure 1.7.2: a sketch of the second circuit to be tested

Finally, the 4-FETs configuration (figure 1.7.3) could be implemented for each coil to have steps in both directions.

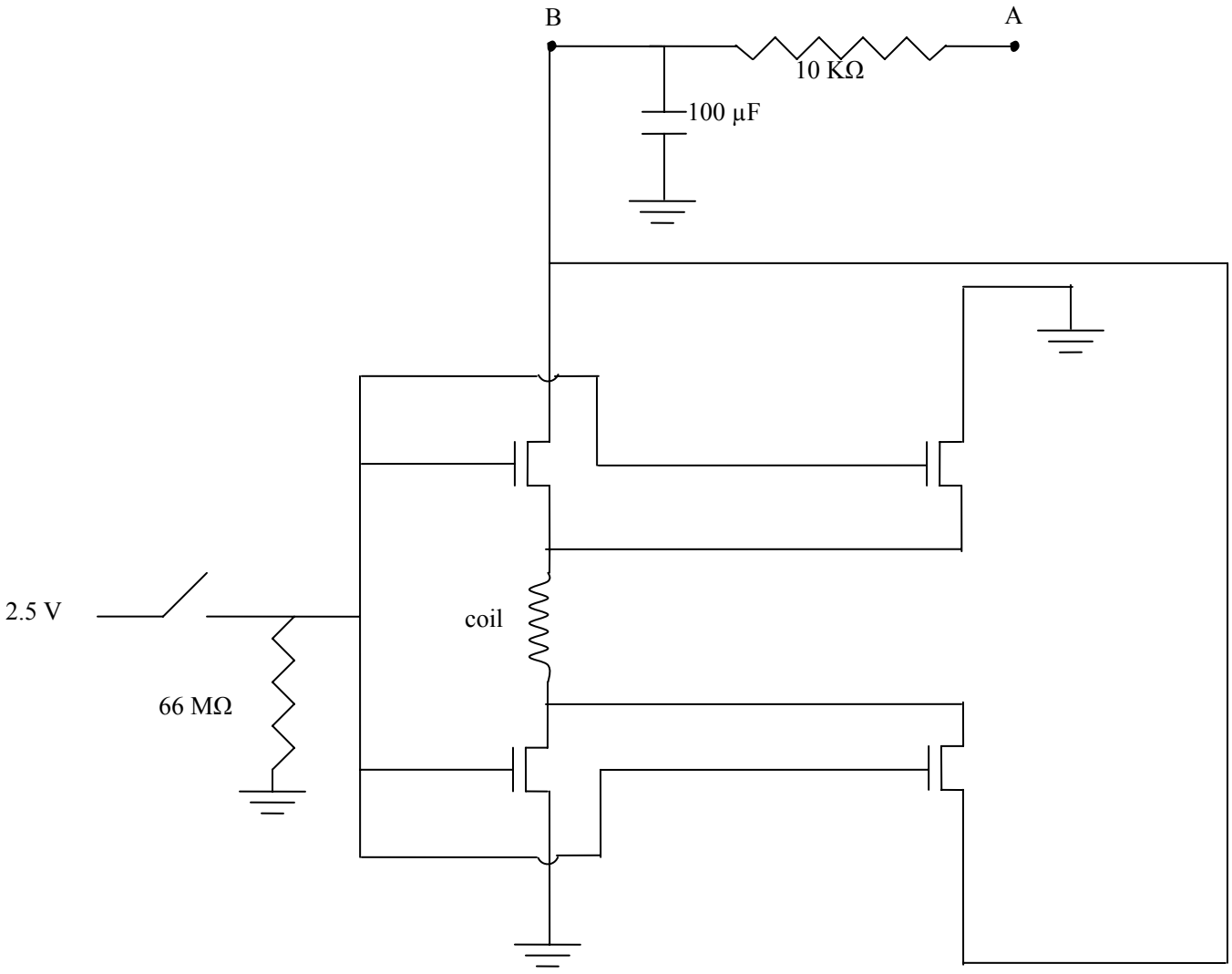

Figure 1.7.3: a sketch of the circuit with four FET switches, so as to inject current into the coil from both directions

After testing the FET configurations, the final step would be to remotely control the FET switches through the frequency of the input laser signal: this task would finally replace the pushbutton switches with a passband filter and a rectifier, as shown in figure 1.7.4, whose components have to be chosen according to the frequency values chosen to drive the motor. A smaller transformer (with a smaller turns ratio, since the gate-source voltage required is small), different from the one used to generate the feed current of the motor, will be placed before the filter, and the rectifier after it, to produce a continuous voltage for the FET gate.

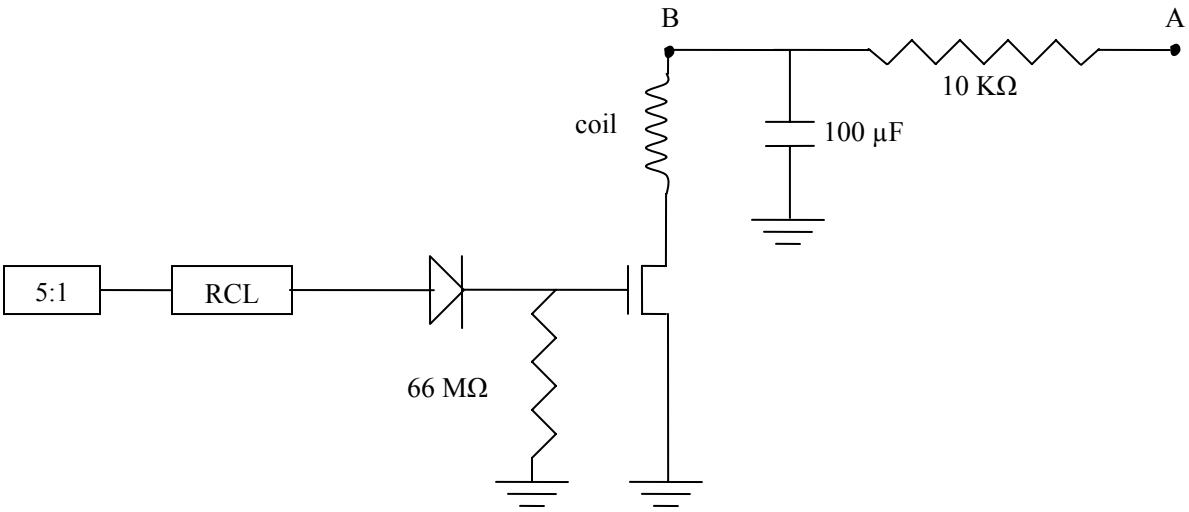

Figure 1.7.3: an illustration of how to replace the pushbutton switch with other components to control the steps through the frequency of the input signal

1.7 IMPROVEMENTS AND NEXT STEPS

Several improvements can be done to improve the system: the transformer used gives a good voltage, but it's not optimized. A better transformer could produce a higher voltage, allowing a smaller capacitor to be used or a faster charge up time. Moreover, problems related to impedance mismatching should be taken into account for a further improvement of the whole system. Finally, a laser with a larger power can be used to provide a stronger signal and surely to lower the waiting time for one step.
The next step will be to practically implement the control circuit. Theoretical considerations have been already illustrated, as well as a few tests still to be done, and the optimal values of each component still have to be figured out. Many other problems will surely arise while implementing the circuit, or some other ways, easier or more convenient that these, could be found to control the stepping motor through the frequency of the input signal.

References

[1]: M. P. Clarizia, “Wireless optical controls of Ligo static suspensions actuators”, available at: http://www.ligo.caltech.edu/~desalvo/Clarizia-Seminar-22.9.05.ppt

[2]: http://en.wikipedia.org/wiki/Stepper_motor

[3]: http://www.vacuumtechnical.com/AML/B232.html

[4]: S. V. Kulkarni, S. A. Khaparde, *Transformer Engineering Design & Practice*, Marcel Dekker, Inc., New York, 2004.

Acknoledgements

Riccardo De Salvo, Calum Torrie, Innocenzo Pinto, Dave Grimmett, Paul Russel, Marco G. Tarallo, Ilaria Taurasi, Yuri Agresti and all the italian people, SFP office, SURF program, United States.